Frontiers of Information Technology & Electronic Engineering
www.jzus.zju.edu.cn; engineering.cae.cn; www.springerlink.com
ISSN 2095-9184 (print); ISSN 2095-9230 (online)
E-mail: jzus@zju.edu.cn

Evaluating acoustic communication performance of micro autonomous underwater vehicles in confined spaces*

Qiu-yang TAO[1], Yue-hai ZHOU[2], Feng TONG[2], Ai-jun SONG[3], Fumin ZHANG[†‡1]

[1]*School of Electrical and Computer Engineering, Georgia Institute of Technology, Atlanta, GA 30332, USA*

[2]*College of Ocean and Earth Sciences, Xiamen University, Xiamen 361005, China*

[3]*Department of Electrical and Computer Engineering, The University of Alabama, Tuscaloosa, AL 35487, USA*

[†]E-mail: fumin@gatech.edu

Received Dec. 14, 2017; Revision accepted July 1, 2018; Crosschecked Aug. 15, 2018

Abstract: Micro-sized autonomous underwater vehicles (μAUVs) are well suited to various applications in confined underwater spaces. Acoustic communication is required for many application scenarios of μAUVs to enable data transmission without surfacing. This paper presents the integration of a compact acoustic communication device with a μAUV prototype. Packet reception rate (PRR) and bit error rate (BER) of the acoustic communication link are evaluated in a confined pool environment through experiments while the μAUV is either stationary or moving. We pinpoint several major factors that impact the communication performance. Experimental results show that the multi-path effect significantly affects the synchronization signals of the communication device. The relative motion between the vehicle and the base station also degrades the communication performance. These results suggest future methods towards improvements.

Key words: Autonomous underwater vehicles; Underwater acoustic communications; Confined water space
https://doi.org/10.1631/FITEE.1700841 **CLC number:** TB567

1 Introduction

Miniaturization is one of the major technology trends in autonomous underwater vehicles (AUVs) (Brun, 2012). Micro-sized AUVs or μAUVs have exclusive advantages of cost efficiency, unparalleled mobility, and capability of applications in confined water spaces. μAUVs have received increasing attention owing to their broad potential including environmental monitoring, infrastructure inspection, underwater human-robot interaction, aquaculture, and fisheries. With compact size and low cost, μAUVs can be scaled to swarm applications, allowing parallelizing of the tasks and providing redundancy for fault tolerance (Osterloh et al., 2012; Mintchev et al., 2014).

Many application scenarios of μAUVs require underwater communication for rapid data transmission without vehicle surfacing (Renner and Golkowski, 2016). Communication links to the central station and between vehicles will help monitor the mission, control the robots, and allow coordination among AUVs (Freitag et al., 2005). In the literature, we present novel solutions to underwater communication between μAUVs with constrained power consumption, size, and cost. Radio and optical communications are the most commonly adopted approaches. However, the range of radio communication is very limited due to heavy attenuation of radio signals (Schill et al., 2004), while optical communication depends on

‡ Corresponding author

* Project supported by the Office of Naval Research (No. N00014-16-1-2667) and the National Natural Science Foundation of China (Nos. 61673370 and 11574258)

ORCID: Fumin ZHANG, https://orcid.org/0000-0003-4428-0537

the clarity of the water (Cochenour et al., 2006; Anguita et al., 2011). In contrast, underwater acoustic communication incorporates sound waves to transmit signals over a much longer distance (Akyildiz et al., 2005). Acoustic communication is a proven technology (Che et al., 2010) and is the only practical method for long-range data transmission underwater (Partan et al., 2007). Acoustic communication has wide application in larger-sized AUVs, including control (Marques et al., 2007), multiple AUV formation (Edwards et al., 2004), coordination tasking (Brignone et al., 2009; Wu et al., 2014), and networking (Freitag et al., 2005).

A significant amount of research has been conducted in the field of underwater acoustic communication. Many factors that may potentially impact the underwater acoustic channel have long been known, including multipath, Doppler shift, reverberation, and tidal variability (Stojanovic et al., 1995; Kilfoyle and Baggeroer, 2000; Akyildiz et al., 2005; Stojanovic et al., 2009; Cho et al., 2016). Intensive efforts on, for instance, channel equalization, Doppler tracking and compensation, have been developed to improve the performance of acoustic communication under non-ideal conditions (Johnson et al., 1997; Sharif et al., 2000; Chitre et al., 2008). Moreover, experiments with AUVs in shallow water (less than 12 m) were demonstrated (Freitag et al., 2000). However, most work on acoustic communication focuses on larger-scale submersibles, and very few projects address applications for low-cost μAUVs. Challenges, including integrating physical devices with the robot, limit the application of acoustic communication on μAUVs. Renner and Golkowski (2016) discussed the limitations of integrating commercially available and academia-built acoustic modems with μAUVs, presented an acoustic modem that was specifically designed for μAUVs, and evaluated the performance of the modem. In addition, Meyer et al. (2017) evaluated the reception rate and ranging accuracy between two μAUVs with onboard acoustic modems. However, these two experiments were carried out in a less confined lake environment while the μAUV was not moving.

In this work, we evaluate both the impact of a constrained pool environment and the motion of a μAUV on the packet reception rate (PRR) and bit error rate (BER) of acoustic communication, and discuss the potential sources of disturbance as well as the possible improvements.

2 System design of μAUV

To facilitate cost-effective lab-based experiments on underwater autonomy, we develop the Georgia-Tech miniature underwater robot (GT-MUR), a multi-purpose μAUV prototype. The simplified structure and convenient features of the GT-MUR significantly reduce the time needed for preparation and maintenance in experiments. With compact size, as shown in Fig. 1, the entire system of the GT-MUR can be transported and deployed in confined areas.

Fig. 1 GT-MUR and the confined pool environment. The μAUV system can be transported with a compact toolbox

System overview: Fig. 2 and Table 1 show the functional block diagram and key specifications of the GT-MUR, respectively. The modularized design of the system is highly flexible and expandable. In addition, the general-purpose x86 onboard computer assures compatibility for integrating new devices and reusing existing software.

Table 1 Key specifications of the GT-MUR

Parameter	Value
Total length	304.8 mm/12.00 inches
Total width	248.1 mm/9.77 inches
Total height	162.0 mm/6.38 inches
Total weight	2.7 kg/5.95 lbs (in air)
Tested depth	10 m/32.8 feet
Battery life	About 2 h
Cost*	About 800 USD

* The cost does not include the base station laptop, nor the acoustic communication devices

Acoustic modem architecture: Fig. 3 shows an acoustic modem, a directional transducer, and an omnidirectional transducer. The modem is stacked with four electronic boards for reduced size. Fig. 4 and Table 2 show the hardware functional diagram and key specifications of the modem, respectively. In addition to the features, including miniature size, the acoustic modem supports ranging and networking, which are highly applicable for μAUV applications (Jiang et al., 2016).

Modulation and demodulation: Direct sequence spectrum (DSSS) modulation is incorporated for robust and interference-resistant transmission. Fig. 5 demonstrates the block diagram of the modulation and demodulation processes.

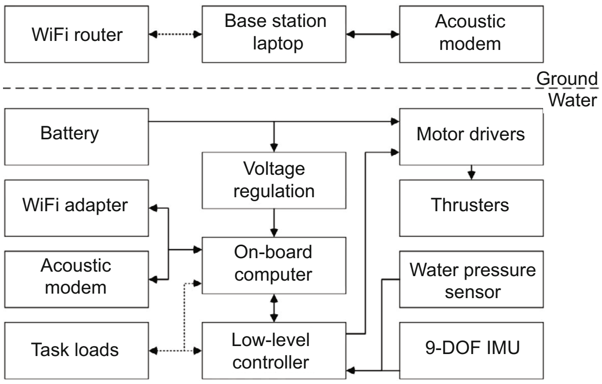

Fig. 2 Functional block diagram of the μAUV prototype, the GT-MUR

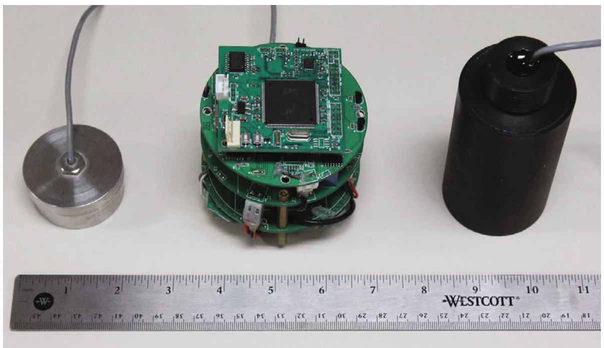

Fig. 3 Acoustic modem (middle) with a directional (left) and an omnidirectional transducer (right). Markings on the top of the ruler are in inches

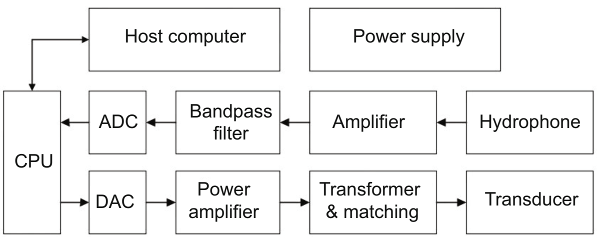

Fig. 4 Functional block diagram of the acoustic communication system

To modulate the binary source message received from the host computer, convolution coding with generator polynomial (171, 133) and coding rate 1/2 is adopted. The coded message is then mapped with two bits, where 00, 01, 10, and 11 are mapped as 0, 1, 2, and 3, respectively. Four orthogonal PN (pseudorandom noise) sequences with center frequency 12.5 kHz, namely PN0, PN1, PN2, and PN3, are chosen for the mapped symbols.

For demodulation, each received symbol is correlated with local PN sequences to obtain the best matching index, thus 0, 1, 2, and 3. The indices are de-mapped to extract the two-bit coded messages, and the messages are then decoded to obtain the binary source.

Signal frame: From the schematic drawing of the signal frame in Fig. 6, the signal frame begins with 10 densely packed synchronization signals. Then, one additional synchronization signal is sent with guarding periods to separate it from the header and the message load. If the synchronization is

Table 2 Key specifications of the acoustic modem

Parameter	Value
Dimension (D/H)	80 mm/100 mm
Speed rate	55 bits/s, configurable
Central frequency	12.5 kHz, configurable
Carrier frequency range	11–14 kHz, configurable
Modulation	DSSS
Communication range*	200 m
Interface to host	RS232/RS485
Base station transducer	Omnidirectional
Onboard transducer	Directional, 60° cone
Length of PN sequence	36.36 ms

* Communication range depends on various factors, including configurable TX power, type of transducer, and the operating environment

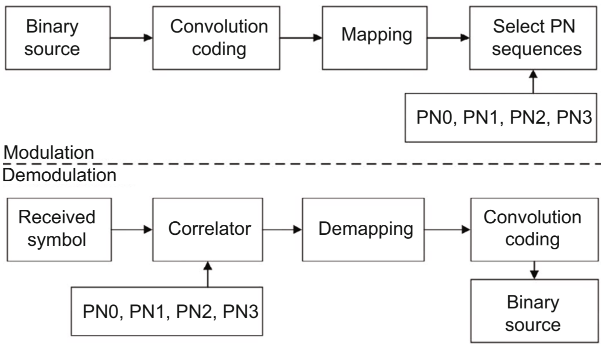

Fig. 5 Modulation and demodulation of the acoustic modem

unsuccessful, the message load will not be demodulated, which will cause packet loss. However, if the synchronization is inaccurate, the message is still able to arrive at the receiver end, but might have error bits.

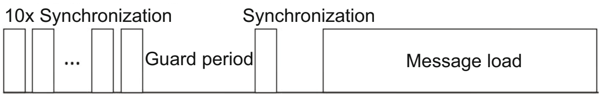

Fig. 6 Signal frame of the acoustic modem. The length of the message load is shortened for better demonstration

Integration on GT-MUR: In Fig. 7, the acoustic modem is installed inside the front section of the GT-MUR while the acoustic transducer is mounted beneath the vehicle. The modem supports the RS232 interface and is connected to the USB port of the host computer via a miniature RS232-to-USB adapter. To reduce complexity and cost, the modem shares a single battery with all onboard electronics. Variation of the battery voltage is regulated by the DC-DC power converter integrated on the acoustic modem.

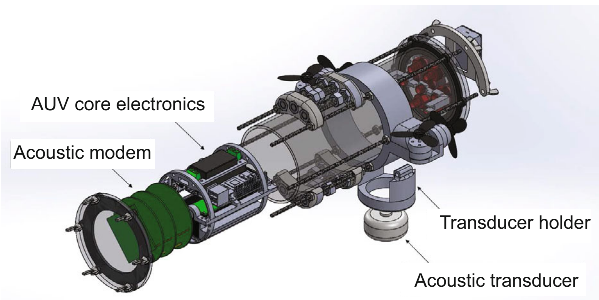

Fig. 7 Integration of an acoustic modem and a transducer with the GT-MUR

Due to the miniature size of the GT-MUR, a compact directional acoustic transducer is integrated on the μAUV while an omnidirectional transducer is deployed on the base station. The onboard directional transducer is installed on the GT-MUR with a 3D printed holder. The onboard transducer is mounted facing downward, which may aggravate any undesired multipath effect by pointing the sound beam towards the bottom of the water area. Experiments conducted to evaluate the communication performance with this configuration are discussed in the following section.

3 Stationary transmission tests

We evaluated the impact of different positions of the μAUV on acoustic communication in a confined water space.

3.1 Experimental setup

A small swimming pool, as shown in Fig. 1, was chosen to represent typical operating environments of many application scenarios of μAUVs, including underwater human-robot interaction and infrastructure inspection. Water was fresh and clear in the pool, with temperature around 17 °C when the experiment was conducted. Fig. 8 shows the detailed dimensions of the swimming pool. On the plot, coordinate O-XY is defined for the convenience of representing positions in the pool.

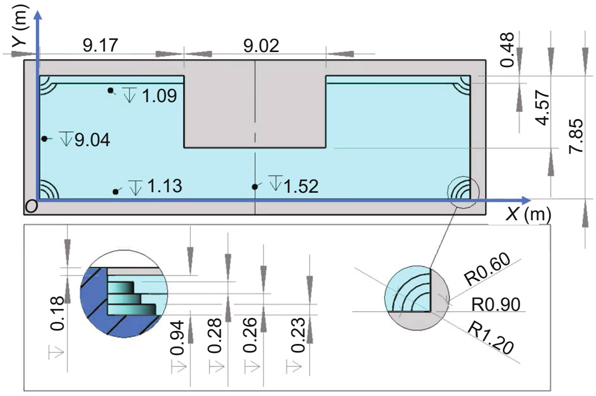

Fig. 8 Dimension of the confined swimming pool

A pair of acoustic modems discussed in Section 2 were deployed on the base station and the μAUV with identical specifications. Packet size and speed rate were set to 48 bytes and 55 bits/s for both modems. As presented in Section 2, a directional acoustic transducer (60° cone) was mounted on the μAUV while an omnidirectional transducer was installed at the base station. The base station transducer was placed at position (4.5, 0.5), with its center located 50 cm below water. On the robot side, we kept the μAUV at a constant depth, where the output surface of the onboard transducer was 50 cm below the water surface (Fig. 9).

Thirteen representative positions were selected throughout the swimming pool. For convenience, the positions are numbered and illustrated as colored squares in Fig. 10. Detailed coordinates of each selected position are listed in Table 3.

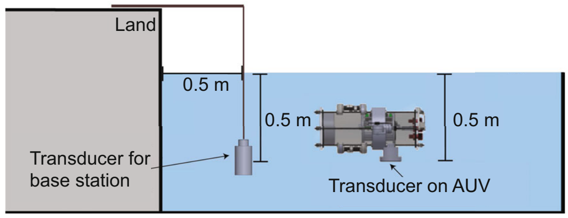

Fig. 9 Depth of the acoustic transducers of the μAUV and the base station

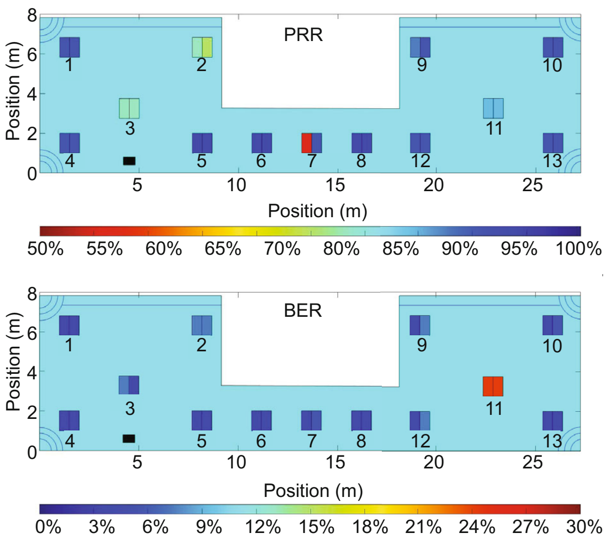

Fig. 10 Packet reception rate (PRR) and bit error rate (BER) of the stationary test. Left (or right) half of each square represents the BER and PER while the μAUV receives packets from (or sends packets to) the base station. The base station transducer is illustrated as a solid black square at the bottom left corner

Table 3 Selected positions for the stationary test

Position index	X (m)	Y (m)	Distance (m)
1	1.50	6.35	6.57
2	8.17	6.33	6.90
3	4.50	3.25	2.78
4	1.50	1.50	3.16
5	8.17	1.50	3.80
6	11.17	1.50	6.74
7	13.68	1.50	9.24
8	16.20	1.50	11.74
9	19.20	6.35	15.82
10	25.87	6.35	22.15
11	25.87	3.28	18.58
12	19.20	1.50	14.73
13	25.87	1.50	21.39

At each selected position, 100 messages were sent from the GT-MUR to the base station, and vice versa. The messages were sent every 15 s to allow the sound of the previous transmission to be damped out. PRR and BER were evaluated as the criteria of acoustic communication performance. Both PRR and BER were calculated at the data link layer of the ISO/OSI model, without medium access control (MAC), acknowledgment, or retries.

3.2 Results and observations

PRR and BER at the selected positions are listed in Table 4 and visualized in Fig. 10 with the drawing of the pool. From the results, we observe that the position of the GT-MUR impacts PRR and BER with the following patterns:

1. Distance has insignificant impact

The distance between the μAUV and the base station transducer has no obvious impact on PRR or BER of the acoustic communication. This observation could be explained by the constrained size of the swimming pool. The largest distance between the selected positions and the base station transducer is only 22.15 m. Therefore, the signal-to-noise ratio (SNR) is not a limiting factor in the entire area of the pool.

In Fig. 9, the directional transducer on the GT-MUR is pointing downward and located at the same depth as the base station transducer. Because of this configuration, there is no direct acoustic path between the transmitter and the receiver. However, this lack of LOS path between the μAUV and the base station transducer has no significant influence on PRR or BER because of high SNR associated with the acoustic propagation paths.

Table 4 Results of the stationary test

Position	PRR (%) (dir1/dir2)	BER (%) (dir1/dir2)
1	93/87	0.09/0.52
2	75/78	6.27/5.75
3	80/80	1.31/9.20
4	93/87	0.00/0.00
5	100/100	0.57/0.00
6	100/98	0.51/0.00
7	95/50	3.59/0.00
8	100/100	0.00/0.00
9	90/84	5.60/0.37
10	93/92	2.79/0.00
11	83/83	24.17/24.86
12	92/90	4.44/0.59
13	90/93	0.00/0.00

dir1: μAUV to base station; dir2: base station to μAUV

2. Position of μAUV has dominant impact

The position of the μAUV relative to the boundaries of the pool shows dominant influence on acoustic communication. For instance, PRR and BER are inferior, when the GT-MUR is near the geometric centers of the pool (positions 3, 7, and 11) and close to the corners where there are no stairs (positions 2 and 9). The multipath effect caused by the confined boundaries of the swimming pool may be the cause of this spatially variant disturbance.

3.3 Analysis and validation

Multipath and reverberation: The multipath effect is usually severe in confined and shallow water areas. Reflections from the surface of the water and the walls of the pool cause disturbances to acoustic communication at different positions to varying degrees. Specifically, the multipath effect may cause unsuccessful or inaccurate synchronization of the acoustic communication, which leads to packet loss or transmission error.

Comparison with the lake environment: To validate that multipath is the dominant factor causing interference in the pool environment, we conducted an experiment in a small lake. In Fig. 11, the width of the lake is about 150 m, and the depth is more than 7 m where the GT-MUR is tested; thus, much less multipath effect is expected. From CTD probe measurement, water temperature and density were around 18 °C and 998.7 kg/m^3, respectively, near the position of the μAUV.

As illustrated in Fig. 12, the GT-MUR was tied at one end of the deck while the base station transducer was placed 115 m and 65 m for positions 1 and 2 from the GT-MUR, respectively. With the same setup as discussed in Section 3.1, 50 messages were sent from the GT-MUR to the base station at each distance, and vice versa. For more comparable results, the background noises of both lake and pool environments were recorded. From Fig. 13, noise levels of the two test fields are very similar, and the energy is concentrated at a low frequency range. Given the 11–14 kHz frequency range of the acoustic modem, no obvious interference is expected from the background noise.

Fig. 11 Photo of the less confined lake environment

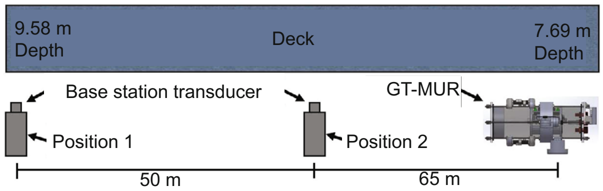

Fig. 12 Setup of the lake experiment

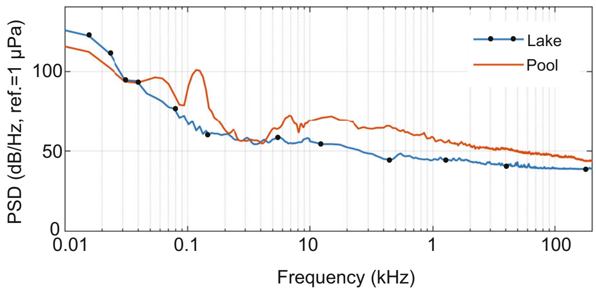

Fig. 13 Power spectral density (PSD) of the background noise from the lake and the swimming pool

PRR and BER of the acoustic transmission test in the lake environment are listed in Table 5, and compared with the averaged results of the experiments conducted in the pool. We observe that, even with a significantly longer distance, PRR and BER in the lake environment are superior to those in the swimming pool. This result shows that multipath effect is the dominant factor impacting the acoustic communication of μAUVs in a confined pool environment.

Table 5 Results of the stationary test in lake

Position	PPR (%) (dir1/dir2)	BER (%) (dir1/dir2)
Pool average, 11 m distance	91/86	3.80/3.44
Lake, 65 m distance	94/96	0.00/0.00
Lake, 115 m distance	94/92	2.34/7.95

dir1: μAUV to base station; dir2: base station to μAUV

Signal frame analysis: Next we study how the synchronization signals suffer from interference from the multipath effect in the swimming pool. Synchronization signals of the acoustic modem were recorded in both lake and pool environments for comparison. Figs. 14 and 15 show the waveforms of the synchronization signals and channel impulse response of the last synchronization signal, respectively.

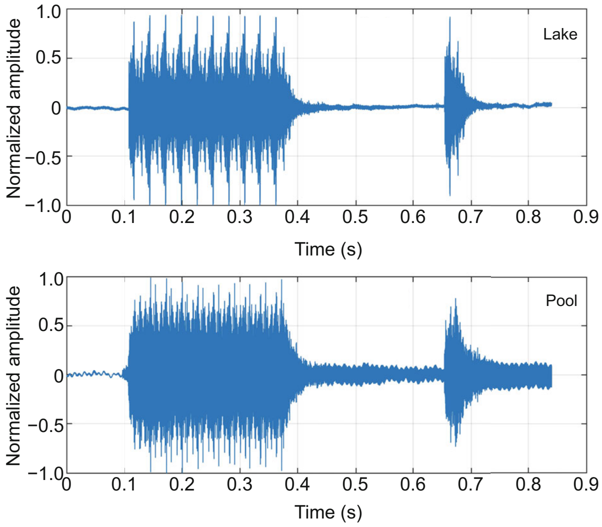

Fig. 14 Synchronization signal of the acoustic modem in lake and pool environments. Waveform during the first 0.1 s is environmental background noise

The reverberations of each synchronization signal cause interference with the subsequent synchronization signals. From the channel impulse response for the last synchronization signal in Fig. 15, we observe that the multipath spread of the pool significantly exceeds that of the lake. In fact, the length of this spread is longer than the 36.36 ms length of the PN sequence used for synchronization signals (Table 2). From the comparison between the synchronization signals in both environments (Figs. 14 and 15), we observe that each synchronization signal takes extra time to attenuate in the swimming pool due to heavy multipath effect. Moreover, as illustrated in Fig. 16, larger fluctuations of multipath channel impulse response are observed in the swimming pool environment.

3.4 Conclusions and discussion

From the experiments and waveform comparison, we conclude that the multipath effect is the dominant factor impacting the acoustic communication in confined water areas. Specifically, reverberations resulting from the multipath effect interfere the synchronization signals, causing inferior communication performance. As a consequence, the quality of the acoustic channel is spatially variant, and depends on the geometry of the confined water area.

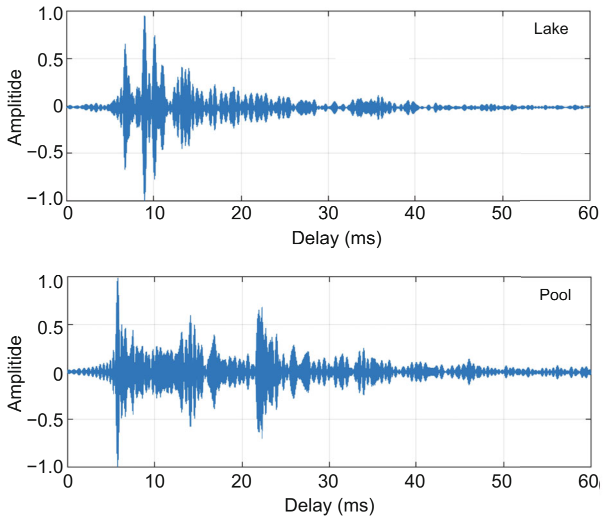

Fig. 15 Channel impulse response of the last (11^{th}) synchronization signal

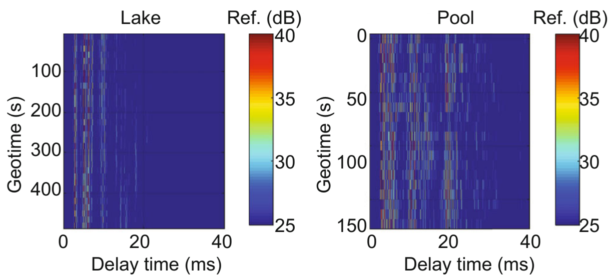

Fig. 16 Fluctuations of multipath channel impulse response in both lake and swimming pool environments

The following proposals could be considered to improve acoustic communication for μAUVs operating in confined spaces: (1) increase the separation among the synchronization signals to tolerate interference from reverberations; (2) since the disturbance of the multipath effect is spatially variant, certain areas of the pool may have severe interference, and the 'blind spots' can be considered during path planning and task planning of μAUVs.

4 Moving transmission test

This experiment was conducted to evaluate the impact of the motion of μAUVs on acoustic communication. Tests were conducted in the same swimming pool environment as discussed in Section 3.1.

4.1 Experimental setup

All experiment setups were identical to those in the stationary test except that the GT-MUR was traveling horizontally. In Fig. 17, four trajectories, denoted by T1 to T4, are defined for the representative scenario that the μAUV is moving towards (T1) or away (T2) from the base station transducer, or is passing the transducer from the left (T3) or the right (T4).

PRR and BER were evaluated by commanding the GT-MUR to travel 50 times along each trajectory. Before each travel began, the GT-MUR was stationary at a predetermined starting position with all motors turned off. About 2 s after the motors were turned on, the GT-MUR started to send one message to the base station. Around 3 s after the acoustic modem finished transmitting, motors were turned off. This procedure is shown in Fig. 17, where the colored lines represent the portions of the trajectories while the modem is transmitting, and the black lines demonstrate the part where the motors are running without acoustic transmission.

Considering the limited size of the swimming pool and relatively long time needed to transmit one message via the acoustic modem, thrusters were commanded at low throttle (8%) to avoid the GT-MUR colliding with the walls of the pool. This throttle setting propelled the μAUV traveling at an average speed around 0.26 to 0.27 m/s, and the mean speed for each trajectory can be found in Table 6. The position of the GT-MUR was tracked for all 50 travels on each trajectory. Averaged positions where the acoustic modem started and finished transmitting are listed in Table 6 and visualized in Fig. 17.

Table 6 Trajectories of the moving test

Trajectory	(X_i, Y_i) (m)	(X_f, Y_f) (m)	Mean speed (m/s)
T1	(4.50, 2.47)	(4.50, 5.10)	0.27
T2	(4.50, 5.27)	(4.50, 2.67)	0.26
T3	(5.94, 4.00)	(3.36, 4.00)	0.26
T4	(3.43, 4.00)	(6.04, 4.00)	0.27

(X_i, Y_i) and (X_f, Y_f) are the averaged positions where the acoustic modem starts and finishes transmitting

4.2 Results and observations

The PRR and BER for the GT-MUR moving on each trajectory are listed in Table 7 and illustrated in Fig. 17. We observe that the motion of the GT-MUR affects acoustic communication with the following patterns:

1. Motion of μAUV on PRR

The averaged PRR of the four trajectories was lower than the value of positions 1–5 sampled at the left portion of the pool. This observation indicates that the motion of GT-MUR may disturb the synchronization signal, and cause inferior PRR. Findings in Section 3 show that the interference of the multipath effect is spatially variant in the pool. Therefore, an additional experiment was designed for more comparable results (see Section 4.3.2).

2. Direction of motion on BER

The trajectories T1 and T2, on which the GT-MUR traveled towards and away from the base station transducer, have significantly inferior BER than T3 and T4, on which the μAUV passed by the transducer. This indicates that the Doppler effect may have impact on the performance of acoustic communication for μAUVs.

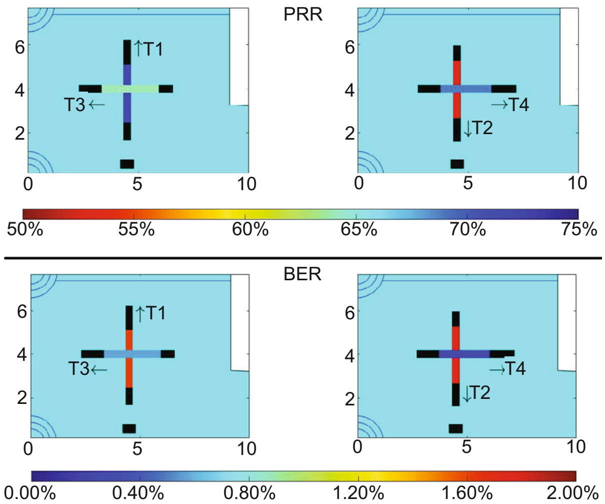

Fig. 17 Packet reception rate (PRR) and bit error rate (BER) in the moving test

4.3 Analysis and validation

Thrusters of the GT-MUR were turned on during this moving experiment, and the noise from the thrusters could potentially impact the acoustic communication. This is in addition to the impact of the

Table 7 Results of the moving test

Trajectory	PRR (%)	BER (%)	Dir
T1	100	0.32	*Y*
T2	58	0.37	*Y*
T3	78	0.10	*X*
T4	86	0.01	*X*

Dir: direction of the trajectory, parallel to the *X* or *Y* axis

movement of the μAUV. Therefore, both self-noise and motion of the GT-MUR were analyzed in this part.

4.3.1 Motor noise

1. Motor noise spectrum

Noise of the thrusters on the GT-MUR was recorded under two operating conditions: (1) Motor throttle swept from 0 to 20%, which is the speed range of the GT-MUR for most application scenarios; (2) Motors ran at constant throttle, 8%, the same speed setting used in the field experiments in this section.

Fig. 18 compares the spectrum of the motors running at constant speed and while they were accelerating. In both cases, frequency of the thruster noise was close to the frequency range of the acoustic modem (11–14 kHz), which indicates that potential interference may exist. Moreover, noise was distributed in a wider frequency range when the motor was accelerating towards 20% throttle, which might cause slightly more interference.

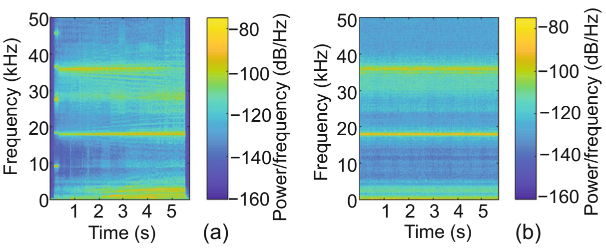

Fig. 18 Spectrum of the thruster noise while the motors are accelerating (a) or running at a constant speed (b)

2. Motors under different conditions

Thrusters with worn motors usually have louder noise than when motors are new. An experiment was designed to evaluate the impact of turning on the thrusters with motors in different conditions. Setups of this test were consistent with those of the moving experiment discussed in Section 4.1, except that the GT-MUR was fixed at position (4.50, 4.00), the intersection of the trajectories T1 to T4. Fifty messages were sent and received while the thrusters were turned off, and commanded at 8% throttle with different motor conditions.

As shown in Table 8, thrusters with new motors had no obvious influence on the acoustic communication, but the aggravated noise from worn motors had noticeable impacts on both PRR and BER. At this point, we would like to point out that new motors were used for all other experiments in this study.

Table 8 Comparison under different motor conditions

Position	PPR (%) (dir1/dir2)	BER (%) (dir1/dir2)
Motor off	100/100	0.00/0.00
New motor	100/100	0.00/0.00
Old motor	94/94	1.08/0.00

dir1: μAUV to base station; dir2: base station to μAUV

3. Conclusion and discussion

From the experiments and analysis, we can conclude that motor noise of the GT-MUR has limited influence on acoustic communication, and is not the dominant disturbance in the moving tests in Section 4.2. Moreover, if the motors are not in good condition, noticeable interference may occur. As indicated in the spectrum of the thruster noise, a slightly heavier impact is expected if the motors are accelerating towards high speeds.

Though the disturbance from motor noise is overall not severe, the following suggestions would help further reduce the interference: (1) Consider noise spectrum of the thrusters while integrating acoustic communication devices. Thrusters with non-overlapping noise spectrum are preferred. (2) For thrusters that have bearings exposed to water, which have been used in many low-cost μAUVs, we suggest checking motor conditions regularly. (3) From our observation during this experiment, the worn and corroded bearing of the motor is the major reason for extra noise. Bearing condition monitoring methods, e.g., the method proposed by Zhou et al. (2007), can be adopted in the future.

4.3.2 Other motion-related factors affecting PRR

In Section 3.3, unsuccessful synchronization may lead to packet loss. The relatively low PRR observed from the experiment described in Section 4.2 indicates that there is heavy loss of synchronization signals.

1. Comparison with stationary transmission

To evaluate the impact of the motion of the GT-MUR on the synchronization signals, an experiment was designed by comparing PRR with the condition in which the μAUV was fixed at a stationary location. Position (4.50, 5.27) was selected for this test as it was the averaged position where the synchronization signals were sent on T2, the trajectory with the lowest PRR. With the same setup as discussed in Section 4.1, 50 messages were sent from the μAUV to the base station, and vice versa.

From Table 9, we observe that the PRR dropped significantly because of the motion of the GT-MUR. Fig. 14 shows that it took about 0.55 s to send all 11 synchronization chips, during which the GT-MUR moved around 14 cm on trajectory T2. This distance was larger than the wavelength of the central frequency (12.5 kHz) of the modem, about 12 cm. From the stationary experiments in Section 3, we know that there was no LOS path due to the configuration of the onboard transducer, and that the multipath effect caused strong spatial variance to the acoustic channel. Therefore, an abrupt change of the acoustic paths may occur while the GT-MUR is traveling, which would lead to unsuccessful synchronizations and thus inferior PRR.

Table 9 Comparison with the μAUV at (4.50, 5.27)

Position	PPR (%)	BER (%)
Stationary, motors on	98	0.00
Moving, motors on	58	0.37

Tests were done with new motors. Motors were commanded at the same speed as in the moving tests

2. Conclusion and discussion

Movement of the μAUV is the dominant factor that affects acoustic communication performance. Specifically, an abrupt change of the acoustic paths (path hopping) causes disturbance to the synchronization signals while the μAUV is moving. An omnidirectional transducer installed on the μAUV would produce a dominant LOS path between the μAUV and the base station, which might reduce the influence of motion on transmission.

4.3.3 Doppler effect on BER

As illustrated in Fig. 17, the BER is higher if the GT-MUR is moving towards and away from the base station transducer. This observation indicates that the Doppler effect may have impact on the acoustic communication. The relative speed between the μAUV and the base station transducer is calculated for each trajectory (Table 10), which shows that the BER becomes significantly inferior if the relative speed gets higher.

Table 10 Relative speed between TX and RX vs. BER

Trajectory	$S_{\max}$ (m/s)	$S_{\min}$ (m/s)	BER (%)
T1	+0.27	+0.27	0.32
T2	–0.26	–0.26	0.37
T3	+0.10	–0.08	0.10
T4	+0.08	–0.11	0.01

$S_{\max}$ and $S_{\min}$ represent the maximum and minimum speeds of the GT-MUR relative to the base station transducer, respectively. Positive value means that the GT-MUR is approaching the base station transducer, and vice versa

Conclusion and suggestion: Because of the limited speed of sound propagating in water, motion induced Doppler distortion is noticeable even when the μAUV is moving at low speed or drifting without intentional motion (Stojanovic et al., 2009). However, by adjusting the planned path of the μAUV, the relative motion between the transducers, and therefore the Doppler effect, could be reduced.

5 Conclusions and future work

This paper presents the integration and performance evaluation of acoustic communication devices on the GT-MUR. Experiments were performed in a confined swimming pool environment while the GT-MUR was stationary and moving to represent typical scenarios of many μAUV applications. The performance of stationary transmission is affected mainly by the multi-path effect of acoustic transmission, which interferes with the synchronization signals used by the acoustic modem. For moving transmission, more factors, including path hopping and the Doppler effect, cause the degradation of performance.

We are planning to further examine the impact of the movement of the GT-MUR on acoustic communication in both the pool and the lake environments. Improvements on the systems will be adopted based on the findings of this study. Specifically, we will adjust the signal frame to tolerate reverberation in a confined water space, use omnidirectional transducers to reduce path hopping caused by movements of the GT-MUR, and plan the motion of the μAUV to maintain good communication performance.

Acknowledgements

The authors would like to express heartfelt gratitude to Sean MAXON, Chang QIN, and Jaeseok CHA for helping with the experiments and building the μAUV prototype.

References

Akyildiz IF, Pompili D, Melodia T, 2005. Underwater acoustic sensor networks: research challenges. *Ad Hoc Netw*, 3(3):257-279. https://doi.org/10.1016/j.adhoc.2005.01.004

Anguita D, Brizzolara D, Parodi G, et al., 2011. Optical wireless underwater communication for AUV: preliminary simulation and experimental results. OCEANS, p.1-5. https://doi.org/10.1109/Oceans-Spain.2011.6003598

Brignone L, Alves J, Opderbecke J, 2009. GREX sea trials: first experiences in multiple underwater vehicle coordination based on acoustic communication. OCEANS, p.1-6. https://doi.org/10.1109/OCEANSE.2009.5278281

Brun LC, 2012. ROV/AUV trends: market and technology. *Mar Technol Rep*, 55(7):48-51. https://doi.org/10.13140/rg.2.1.4062.5686

Che XH, Wells I, Dickers G, et al., 2010. Re-evaluation of RF electromagnetic communication in underwater sensor networks. *IEEE Commun Mag*, 48(12):143-151. https://doi.org/10.1109/MCOM.2010.5673085

Chitre M, Shahabudeen S, Freitag L, et al., 2008. Recent advances in underwater acoustic communications & networking. OCEANS, p.1-10. https://doi.org/10.1109/OCEANS.2008.5289428

Cho S, Zhang FM, Edwards C, 2016. Tidal variability of acoustic detection. IEEE Int Conf on Big Data and Cloud Computing (BDCloud), Social Computing and Networking (SocialCom), Sustainable Computing and Communications (SustainCom), p.431-436. https://doi.org/10.1109/BDCloud-SocialCom-SustainCom.2016.70

Cochenour B, Mullen L, Laux A, et al., 2006. Effects of multiple scattering on the implementation of an underwater wireless optical communications link. OCEANS, p.1-6. https://doi.org/10.1109/OCEANS.2006.306863

Edwards DB, Bean TA, Odell DL, et al., 2004. A leader-follower algorithm for multiple AUV formations. IEEE/OES Autonomous Underwater Vehicles, p.40-46. https://doi.org/10.1109/AUV.2004.1431191

Freitag L, Grund M, Singh S, et al., 2000. Acoustic communication in very shallow water: results from the 1999 AUV Fest. OCEANS MTS/IEEE Conf and Exhibition, p.2155-2160. https://doi.org/10.1109/OCEANS.2000.882253

Freitag L, Grund M, Singh S, et al., 2005. The WHOI micromodem: an acoustic communications and navigation system for multiple platforms. OCEANS MTS/IEEE, p.1086-1092. https://doi.org/10.1109/OCEANS.2005.1639901

Jiang WH, Tong F, Zhou YH, 2016. R&D of an spread spectrum acoustic communication modem with ranging capability. Proc 11th ACM Int Conf on Underwater Networks & Systems, Article 15. http://doi.org/10.1145/2999504.3001109

Johnson M, Freitag L, Stojanovic M, 1997. Improved Doppler tracking and correction for underwater acoustic communications. IEEE Int Conf on Acoustics, Speech, and Signal Processing, p.575-578. https://doi.org/10.1109/ICASSP.1997.599703

Kilfoyle DB, Baggeroer AB, 2000. The state of the art in underwater acoustic telemetry. *IEEE J Ocean Eng*, 25(1):4-27. https://doi.org/10.1109/48.820733

Marques ERB, Pinto J, Kragelund S, et al., 2007. AUV control and communication using underwater acoustic networks. OCEANS, p.1-6. https://doi.org/10.1109/OCEANSE.2007.4302469

Meyer B, Isokeit C, Maehle E, et al., 2017. Using small swarm-capable AUVs for submesoscale eddy measurements in the Baltic Sea. OCEANS MTS/IEEE, p.1-5.

Mintchev S, Donati E, Marrazza S, et al., 2014. Mechatronic design of a miniature underwater robot for swarm operations. IEEE Int Conf on Robotics and Automation, p.2938-2943. https://doi.org/10.1109/ICRA.2014.6907282

Osterloh C, Pionteck T, Maehle E, 2012. MONSUN II: A small and inexpensive AUV for underwater swarms. ROBOTIK; 7th German Conf on Robotics, p.1-6.

Partan J, Kurose J, Levine BN, 2007. A survey of practical issues in underwater networks. *ACM SIGMOBILE Mob Comput Commun Rev*, 11(4):23-33. https://doi.org/10.1145/1347364.1347372

Renner C, Golkowski AJ, 2016. Acoustic modem for micro AUVs: design and practical evaluation. Proc 11th ACM Int Conf on Underwater Networks & Systems, Article 2. https://doi.org/10.1145/2999504.3001076

Schill F, Zimmer UR, Trumpf J, 2004. Visible spectrum optical communication and distance sensing for underwater applications. Australasian Conf on Robotics and Automation, p.1-8.

Sharif BS, Neasham J, Hinton OR, et al., 2000. A computationally efficient Doppler compensation system for underwater acoustic communications. *IEEE J Ocean Eng*, 25(1):52-61. https://doi.org/10.1109/48.820736

Stojanovic M, 1995. Underwater acoustic communications. Proc Electro/Int, p.435-440. https://doi.org/10.1109/ELECTR.1995.471021

Stojanovic M, Preisig J, 2009. Underwater acoustic communication channels: Propagation models and statistical characterization. *IEEE Commun Mag*, 47(1):84-89. https://doi.org/10.1109/MCOM.2009.4752682

Wu WC, Song AJ, Varnell JP, et al., 2014. Cooperatively mapping of the underwater acoustic channel by robot swarms. Proc 9th ACM Int Conf on Underwater Networks & Systems, Article 20. https://doi.org/10.1145/2671490.2674572

Zhou W, Habetler TG, Harley RG, 2007. Bearing condition monitoring methods for electric machines: a general review. IEEE Int Symp on Diagnostics for Electric Machines, Power Electronics and Drives, p.3-6. https://doi.org/10.1109/DEMPED.2007.4393062